

Advanced Training in Neonatal/Perinatal Medicine

EXAMPLE PROJECT

PROJECT TITLE: Dräger VN500's oscillatory performance has a frequency dependent threshold

Abbreviations

1		
2		
3		
4		
5		
6		
7		
8		
9	C_{RS}	Respiratory system compliance
10		
11	ETT	Endotracheal tube
12		
13	Fr	Frequency
14		
15	HFOV	High-frequency oscillatory ventilation
16		
17	Hz	Hertz
18		
19	I:E	Inspiratory to expiratory ratio
20		
21	MAP	Mean airway pressure
22		
23	ΔP	Oscillatory change in pressure
24		
25	P_{AO}	Pressure at the airway opening
26		
27	P_{TRACH}	Pressure in the 'trachea' of the test lung
28		
29	P_{VENT}	Pressure in the ventilator
30		
31	R_{RS}	Respiratory system resistance
32		
33	SM3100	Sensormedics 3100 high-frequency oscillator
34		
35	V_{AO}	Flow at the airway opening
36		
37	VN500	Dräger VN500 high-frequency oscillator
38		
39	V_{THF}	High-frequency tidal volume at the airway opening
40		
41		
42		
43		
44		
45		
46		
47		
48		
49		
50		
51		
52		
53		
54		
55		
56		
57		
58		
59		
60		

1
2
3
4
5
6
7
8
9
10
11
12
13
14
15
16
17
18
19
20
21
22
23
24
25
26
27
28
29
30
31
32
33
34
35
36
37
38
39
40
41
42
43
44
45
46
47
48
49
50
51
52
53
54
55
56
57
58
59
60

What is already known on this topic?

- Safe and effective application of high frequency ventilation requires an understanding of the performance characteristics of the ventilator being used.
- High-frequency ventilators demonstrate differences in their performance characteristics. Some older ventilators are known to have a frequency related limitation in pressure amplitude and tidal volume.

What this paper adds?

- In the benchtop setting, the Dräger VN500 demonstrates a frequency related reduction in oscillatory pressure amplitude not observed in the Sensormedics 3100.
- Increasing the frequency of oscillations resulted in a greater reduction in delivered high-frequency tidal volume in the Dräger VN500 compared with the Sensormedics 3100.
- Clinicians need to be aware of these differences and may need to adapt their ventilation strategies accordingly.

Abstract

Background: The high-frequency pressure amplitude (ΔP) of the Dräger BabyLog 8000 High-frequency ventilator is related to the frequency, and clinical application differs from other high-frequency devices. The performance characteristics of the new VN500 ventilator have not been described.

Aim: To compare the high-frequency pressure amplitude (ΔP) and tidal volume (V_{THF}) delivered by the Dräger VN500 and the Sensormedics 3100 (SM3100) through a range of oscillatory frequencies.

Methods: In this benchtop study high-frequency oscillations were applied to an infant test lung at unrestricted set amplitudes. Pressure and flow were measured as a function of frequency, incremented by 1 Hz from 5 to 15 Hz. Measurements were repeated for a range of ventilator settings, and lung resistive and compliance states.

Results: The VN500, but not the SM3100, demonstrated an exponential decrease in airway opening ΔP as frequency increased. The difference between the SM3100 and VN500 delivered V_{THF} became greater with each frequency increment. At 15Hz, VN500 V_{THF} was 49% of SM3100 V_{THF} .

Conclusions: The VN500 demonstrates a frequency related reduction in ΔP not observed in the SM3100. Clinicians need to be aware of these differences in performance characteristics.

Abstract word count: 186 words

INTRODUCTION

High-frequency oscillatory ventilation (HFOV) is commonly used in neonatal intensive care units. The mechanism of gas exchange during HFOV is complex¹ and may vary according to the method of generation and attenuation of the pressure waveform²⁻⁴.

The Sormedics 3100 (SM3100; CareFusion, San Diego, CA) and BabyLog 8000+ (Drägerwerk Ag & Co., Lübeck, Germany) have been in wide use for more than two decades. The SM3100 uses a piston-diaphragm, where as the BabyLog 8000+ uses a Venturi system to generate oscillatory pressure amplitudes (ΔP) and resultant tidal volumes. In the BL8000+, a frequency dependent maximum ΔP threshold is known to exist⁵. Consequently, different settings are required when ventilating with the BabyLog 8000+ compared with the SM3100. Lower frequencies are used in order to deliver tidal volumes capable of maintaining adequate gas exchange. The VN500 ventilator superseded the BabyLog 8000+ in 2010, reportedly with a more powerful venturi system. The relationship between applied frequency, ΔP and tidal volume for the VN500 have not previously been reported.

The aims of our benchtop study were 1) to determine whether there were differences in the maximal ΔP and tidal volume that could be generated through a range of frequencies and lung compliance and resistance states using the VN500, and 2) compare these with the performance characteristics of the SM3100.

METHODS

Experiment Setup

This study was performed using a variable compliance (C_{RS} ; minimum 1.0 mL/cm H₂O) infant test lung (model 560li, Michigan Instruments, Grand Rapids, MI). Each device was attached via the manufacturer's recommended circuit (VN500; Dräger VentStar Heated N circuit, and SM3100; Carefusion flexible patient circuit) to an uncuffed 2.5mm or 3.5mm endotracheal tube (ETT) trimmed to 15 cm and attached to the test lung to make a leak free system. To minimize the variable effect of humidity, on resistance and ΔP , the humidifier block was removed from the circuits.

Measurements

The experimental arrangement is shown in Figure 1. Airway pressure was measured using pressure transducers (1000Hz; SC-24, SCIREQ, Montreal, Canada) located at the proximal end of the inspiratory limb of the ventilator circuit (P_{VENT}), proximal to the ETT at the airway opening (P_{AO}) and from a dedicated pressure port within the test lung (P_{TRACH}). Flow (V'_{AO}) and tidal volume (V_{THF}) were measured using a hot wire anemometer (200Hz; Florian respiration monitor, Acutronic Medical Systems, Zug, Switzerland) located at the airway opening⁶.

Experiment Protocol

For both the SM3100 and VN500, ventilation was applied with a set ΔP of 90 cm H₂O (maximum setting for VN500) and frequency (Fr) increased in 1 Hz increments every 5 minutes from 5 to 15 Hz. This was performed for all permutations of inspiratory to

1
2
3
4 expiratory ratio (I:E) 1:2 and 1:1, and test lung C_{RS} 1.0 and 2.0 mL/cm H₂O . Airway
5
6 resistance (R_{RS}), was varied by using a 3.5 mm ETT with a mean airway pressure (MAP) of
7
8 20 cm H₂O, and a 2.5 mm ETT (MAP 10 cm H₂O).
9

10 11 12 13 14 **Data Analysis**

15 Pressure and flow signals were digitized using LabChart 7.2 (ADInstruments, Sydney,
16
17 Australia). The amplitude (Δ) of the P_{VENT} , P_{AO} and P_{TRACH} waveforms was calculated for
18
19 the last 300 stable consecutive oscillations at each recording. Each parameter was graphed
20
21 against frequency and the relationship examined to determine the best linear or non-linear
22
23 model using Prism V4.02 (GraphPad, San Diego, CA). The simplest model in which all
24
25 coefficients of determination (R^2) were significant ($p < 0.05$) was deemed representative,
26
27 and a $R^2 > 0.7$ defined as a good fit of the model.
28
29
30
31
32
33
34

35 **RESULTS**

36
37 For the VN500, but not SM3100, ΔP_{VENT} decreased exponentially as the Fr was increased
38
39 from 5 to 15 Hz despite a constant ventilator ΔP set at 90 cm H₂O (Figure 2), irrespective
40
41 of I:E ratio, MAP and ETT size permutations; all $R^2 > 0.95$. The SM3100 maintained a
42
43 stable ΔP_{VENT} approximating the set ΔP at all Fr examined. I:E ratio exerted the greatest
44
45 influence on the absolute ΔP_{VENT} at each Fr in the VN500. At 15 Hz with a I:E ratio of 1:2,
46
47 C_{RS} 1.0 mL/cm H₂O and ETT 2.5mm, the maximum ΔP_{VENT} recorded was 34.2 cm H₂O,
48
49 compared with 41.3 cm H₂O using I:E 1:1, C_{RS} 2.0 mL/cm H₂O and ETT 3.5mm
50
51 (Supplemental Digital Content Figure 1). The relationship between frequency and ΔP_{VENT}
52
53 was similar at different C_{RS} and R_{RS} permutations, except at test lung C_{RS} of 1.0 mL/cm
54
55
56
57
58
59
60

1
2
3
4 H₂O and the lower R_{RS} (3.5 ETT). At these settings, ΔP_{VENT} was 4 to 10 cm H₂O higher
5
6
7 than the other permutations between frequencies of 7 to 13 Hz in the VN500.
8
9

10
11 Figure 3 shows the relationships between Fr and ΔP_{AO} and V_{THF} using the same
12
13 permutations as Figure 2. A similar exponential decrease in ΔP_{AO} in the VN500 was seen
14
15 ($R^2 > 0.97$). There was no change in ΔP_{AO} with the SM3100. Both devices had a similar
16
17 pattern of frequency related decrease in V_{THF} . As Fr was increased, the difference in
18
19 absolute V_{THF} between the SM3100 and VN500 became incrementally greater
20
21 (Supplemental Digital Content Figure 2). By 15 Hz, the V_{THF} delivered by the SM3100B
22
23 was almost twice that of the VN500. The difference in ΔP_{TRACH} between the two oscillators
24
25 as the frequency was increased was similar to that of V_{THF} (Supplemental Digital Content
26
27 Figure 3), with the potential of the VN500 ΔP_{TRACH} being at least 40% less than the
28
29 SM3100B at frequencies of 10 Hz or more (Figure 4 and Supplemental Digital Content
30
31 Figure 4).
32
33
34
35
36
37
38
39
40

41 DISCUSSION

42 In this benchtop study, we found that there was a difference between the new VN500 and
43
44 SM3100 with regards to the delivered V_{THF} and ΔP at various points in the respiratory
45
46 circuit that became more marked as the frequency was increased. I:E ratio, C_{RS} and R_{RS}
47
48 influenced the magnitude of changes observed. Our results are a guide to the theoretical
49
50 maximum ΔP that could be generated at any given frequency. To our knowledge, this is the
51
52 first report of the ΔP performance characteristics of the VN500 in HFOV mode.
53
54
55
56
57
58
59
60

1
2
3
4 The performance characteristics of the SM3100 have been well described previously, and
5 our results are consistent with these studies^{3,5,7,8}. The pattern of performance characteristics
6 we observed in the VN500 shows similarities to those of the BL8000⁵. The VN500 was
7 able to generate larger V_{THF} at higher frequencies than those reported for the BL8000⁵, but
8 these were still closer to the BL8000 than the SM3100. The relationship between set ΔP
9 and ΔP_{VENT} suggests that the frequency dependent relationship we observed relates to the
10 similarities in the underlying mechanism used to generate HFOV in the two Dräger devices,
11 both of which use a Venturi-assisted expiration system as opposed to a piston diaphragm
12 (SM3100). The Venturi system has been attributed to the performance differences in the
13 BL8000. It seems likely that same, albeit more powerful, Venturi-assisted expiration
14 system accounts for the results we observed in the VN500.
15
16
17
18
19
20
21
22
23
24
25
26
27
28
29
30
31
32

33 Alveolar ventilation during HFOV is determined by the product of the frequency and the
34 square of V_{THF} , with V_{THF} representing the stroke volume of the pressure amplitude^{9,10}. The
35 square relationship between alveolar ventilation and V_{THF} suggests that the difference in
36 alveolar ventilation between these two devices is likely to be even greater. Further studies
37 are required to determine whether our findings translate to significant differences in carbon
38 dioxide removal at higher frequencies.
39
40
41
42
43
44
45
46
47
48

49 The optimal set frequency is determined by the pathophysiology and resultant time constant
50 of the lung¹¹. Unlike the SM3100, there appears to be limits in the ΔP that the VN500 could
51 be expected to achieve at certain frequencies. In Australasia, HFOV is used for those
52 infants with the most severe respiratory failure¹². In these situations, clinicians may need to
53
54
55
56
57
58
59
60

1
2
3
4 decrease frequency and/or increase I:E ratio with the VN500 to achieve adequate ΔP and
5
6 V_{THF} for CO_2 removal. Clinicians need to be aware that unlike conventional ventilation
7
8 where settings are largely interchangeable between ventilators, in HFOV devices the
9
10 settings are unique to the device and are not transferable.
11
12
13
14

15
16 We chose a ΔP of 90 cm H_2O , well above settings being used clinically, to allow
17
18 unrestricted performance of the oscillator. This was intentional, as this is the first report of
19
20 the performance characteristics of the VN500. Choosing a lower ΔP setting may have
21
22 applied an external limitation on performance, and misrepresented the inherent technical
23
24 capabilities of each device. By allowing unrestricted performance of the high-frequency
25
26 power we were also able to inform the clinician of the theoretical maximum ΔP that could
27
28 be expected from the VN500 at any given frequency. It is likely that other more variable
29
30 factors, such as leak, water in the circuit (humidification), spontaneous respiratory effort
31
32 and nature of lung pathology would exert a negative rather than positive effect on our
33
34 findings.
35
36
37
38
39
40
41

42 This study has a number of limitations. This was a benchtop study and the findings may not
43
44 be clinically transferable. Minimum simulated C_{RS} was limited to 1.0 mL/cm H_2O , greater
45
46 than in severe lung disease. Differences in patient circuits can attenuate high-frequency
47
48 oscillations; the rigid SM3100 circuit has low R_{RS} , and differs from the VN500 circuit.
49
50 Nonetheless, some of the frequency related performance characteristics we observed were
51
52 also noted upstream from the circuit. This suggests that our findings relate to the inherent
53
54 operational characteristics of these devices.
55
56
57
58
59
60

1
2
3
4
5
6
7 **Conclusions**

8
9 Like the BL8000, set frequency and I:E ratio determine the maximum ΔP available in the
10
11 VN500. Clinicians need to be aware of the properties of their high-frequency ventilators
12
13 and adapt their ventilation strategies accordingly.
14
15

16
17
18
19 **ACKNOWLEDGEMENTS**

20
21 The authors gratefully acknowledge [redacted] and [redacted] for advice on
22
23 this study, Dräger Medical for use of the Dräger VN500.
24
25
26
27
28
29
30
31
32
33
34
35
36
37
38
39
40
41
42
43
44
45
46
47
48
49
50
51
52
53
54
55
56
57
58
59
60

REFERENCES

1. Slutsky AS, Drazen JM. Ventilation with Small Tidal Volumes. *N Engl J Med* 2002;347:630-1.
2. Thome U, Pohlandt F. Effect of the TI/TE ratio on mean intratracheal pressure in high-frequency oscillatory ventilation. *J Appl Physiol* 1998;84:1520-7.
3. Pillow J, Wilkinson MH, Neil HL, Ramsden CA. In vitro performance characteristics of high-frequency oscillatory ventilators. *Am J Respir Crit Care Med* 2001;164:1019-24.
4. Gerstmann DR, Fouke JM, Winter DC, Taylor AF, A deLemos R. Proximal, tracheal, and alveolar pressures during high-frequency oscillatory ventilation in a normal rabbit model. *Pediatr Res* 1990;28:367-73.
5. Jouvet P, Hubert P, Isabey D, Pinquier D, Dahan E, Cloup M, et al. Assessment of high-frequency neonatal ventilator performances. *Intensive Care Med* 1997;23:208-13.
6. Scalfaro P, Pillow JJ, Sly PD, Cotting J. Reliable tidal volume estimates at the airway opening with an infant monitor during high-frequency oscillatory ventilation. *Crit Care Med* 2001;29:1925-30.
7. Hatcher D, Watanabe H, Ashbury T, Vincent S, Fisher J, Froese A. Mechanical performance of clinically available, neonatal, high-frequency, oscillatory-type ventilators. *Crit Care Med* 1998;26:1081-8.
8. Laubscher B, Greenough A, Costeloe K. Performance of high frequency oscillators. *British Journal of Intensive Care* 1996;6:148-54.
9. Chang HK. Mechanisms of gas transport during ventilation by high-frequency oscillation *J Appl Physiol* 1984;56: 553-563.
10. Froese AB. High frequency ventilation. *Can J Anaesth* 1987;34:37-40.
11. Venegas JG, Fredberg JJ. Understanding the pressure cost of ventilation: why does high-frequency ventilation work? *Crit Care Med* 1994;22:S49.

1
2
3
4
5
6
7
8
9
10
11
12
13
14
15
16
17
18
19
20
21
22
23
24
25
26
27
28
29
30
31
32
33
34
35
36
37
38
39
40
41
42
43
44
45
46
47
48
49
50
51
52
53
54
55
56
57
58
59
60

12. Tingay DG, Mills JF, Morley CJ, Pellicano A, Dargaville PA. Trends in use and outcome of newborn infants treated with high frequency ventilation in Australia and New Zealand, 1996-2003. *J Paediatr Child Health* 2007;43:160-166.

FIGURE LEGENDS

Figure 1. Schematic diagram of the experimental setup. Pressure transducers are shown as dark grey squares. Flow (V_{AO} ; black square) was measured at the airway opening between the ETT and the ventilator hot wire anemometer (VN500) or sham anemometer (SM3100B).

Figure 2. Relationship between frequency and ΔP_{VENT} for the SM3100 (diamonds) and VN500 (circles) at 1:1 (closed symbols and dashed lines) and 1:2 (open symbols and solid lines) I:E ratio. Data shown for a test lung C_{RS} of 1.0 mL/cm H₂O, ETT 2.5mm and mean airway pressure 10 cm H₂O. Other permutations are provided in the online supplemental material.

Figure 3. A. Relationship between frequency and ΔP_{AO} for the SM3100 (diamonds) and VN500 (circles) at a test lung C_{RS} of 1.0 mL/cm H₂O and 2.5 mm ETT. **B.** Relationship between frequency and V_{THF} for the SM3100 (triangles) and VN500 (squares) at the same settings. For both relationships data is shown for I:E ratios of 1:1 (closed symbols and dashed lines) and 1:2 (open symbols and solid lines). There was no difference in the relationships for the other permutations with a 2.5 mm ETT. The 3.5 mm ETT data is available in the online supplemental material.

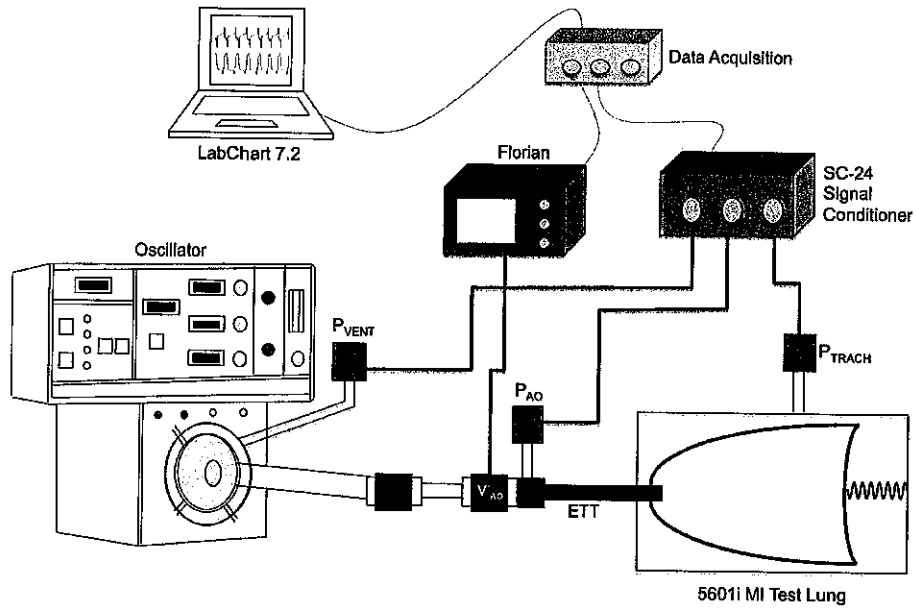
1
2
3
4
5
6
7
8
9
10
11
12
13
14
15
16
17
18
19
20
21
22
23
24
25
26
27
28
29
30
31
32
33
34
35
36
37
38
39
40
41
42
43
44
45
46
47
48
49
50
51
52
53
54
55
56
57
58
59
60

Figure 4. Percentage difference in ΔP_{TRACH} generated by the SM3100 and VN500 at different frequencies in a test lung with C_{RS} 1.0 mL/cm H₂O and 2.5 mm ETT. Closed circles represent data for I:E ratio of 1:1 and open circles 1:2.

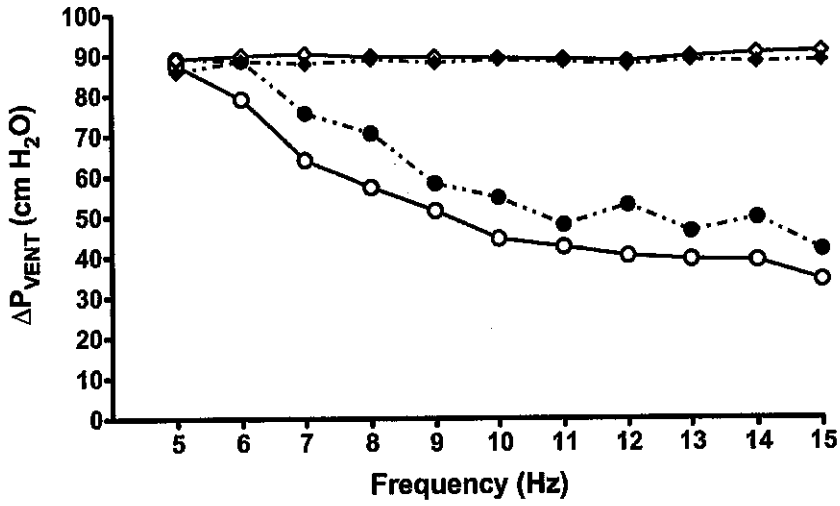




1
2
3
4
5
6
7
8
9
10
11
12
13
14
15
16
17
18
19
20
21
22
23
24
25
26
27
28
29
30
31
32
33
34
35
36
37
38
39
40
41
42
43
44
45
46
47
48
49
50
51
52
53
54
55
56
57
58
59
60



260x166mm (150 x 150 DPI)

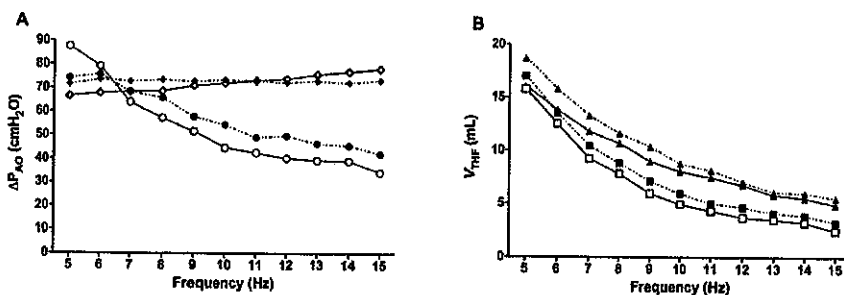


122x72mm (300 x 300 DPI)

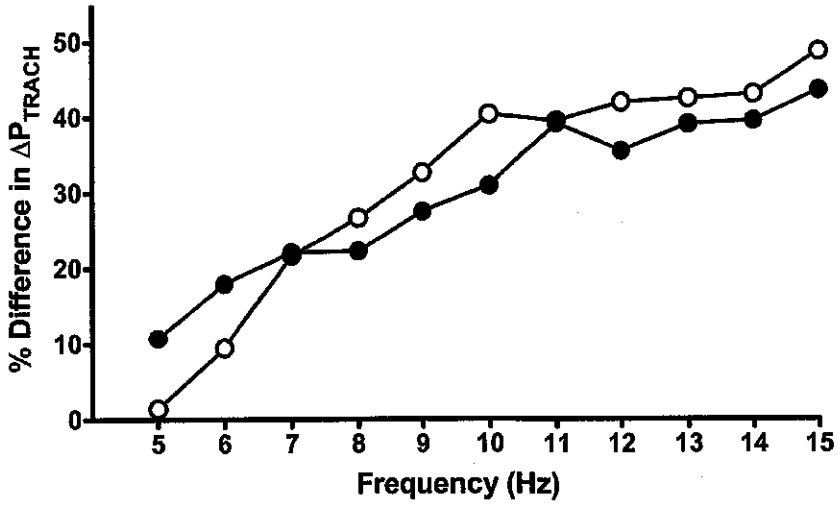
1
2
3
4
5
6
7
8
9
10
11
12
13
14
15
16
17
18
19
20
21
22
23
24
25
26
27
28
29
30
31
32
33
34
35
36
37
38
39
40
41
42
43
44
45
46
47
48
49
50
51
52
53
54
55
56
57
58
59
60



1
2
3
4
5
6
7
8
9
10
11
12
13
14
15
16
17
18
19
20
21
22
23
24
25
26
27
28
29
30
31
32
33
34
35
36
37
38
39
40
41
42
43
44
45
46
47
48
49
50
51
52
53
54
55
56
57
58
59
60



86x29mm (300 x 300 DPI)



122x73mm (300 x 300 DPI)

1
2
3
4
5
6
7
8
9
10
11
12
13
14
15
16
17
18
19
20
21
22
23
24
25
26
27
28
29
30
31
32
33
34
35
36
37
38
39
40
41
42
43
44
45
46
47
48
49
50
51
52
53
54
55
56
57
58
59
60

ONLINE SUPPLEMENTAL MATERIAL

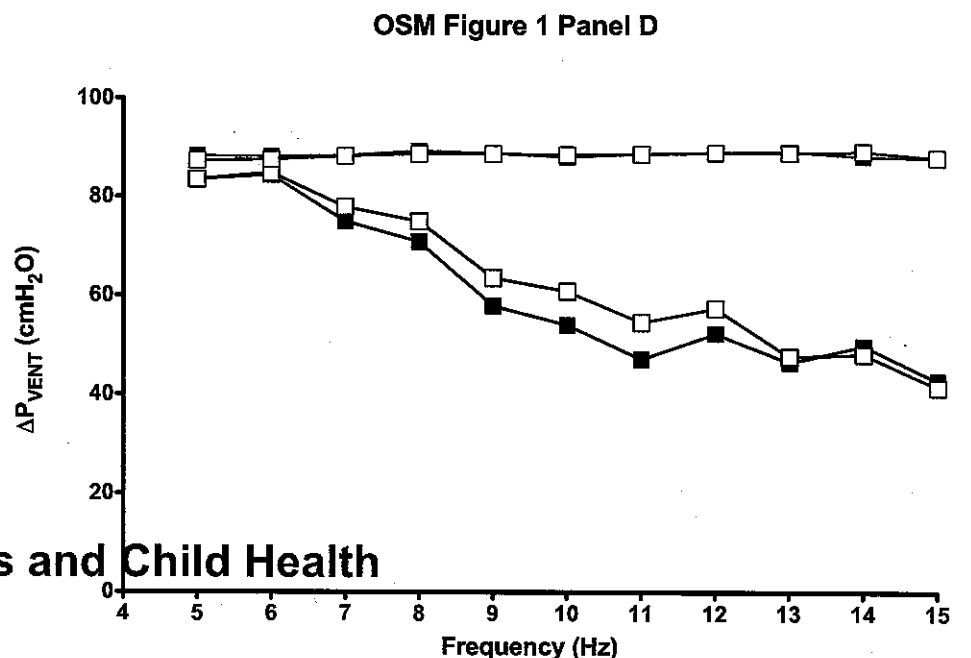
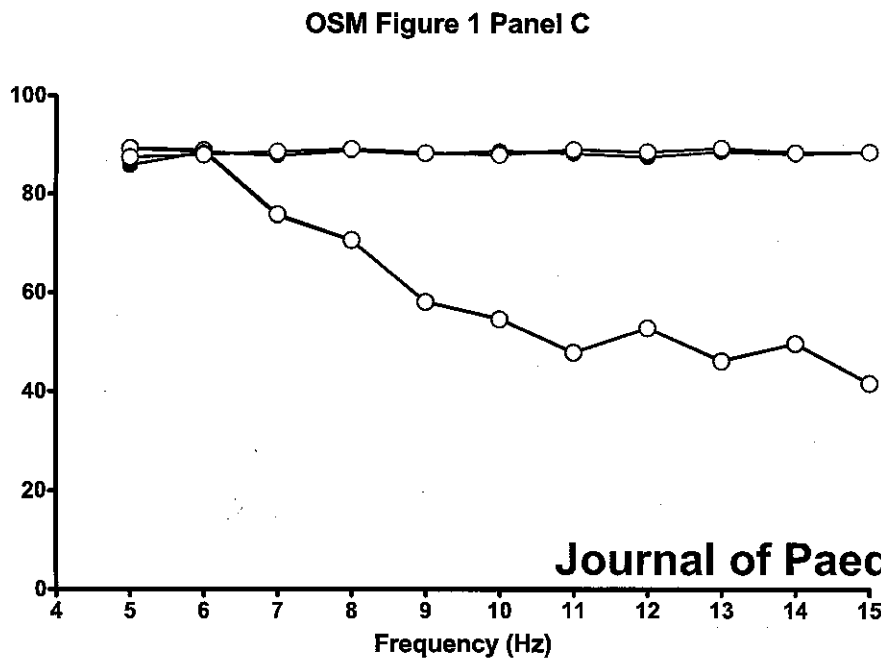
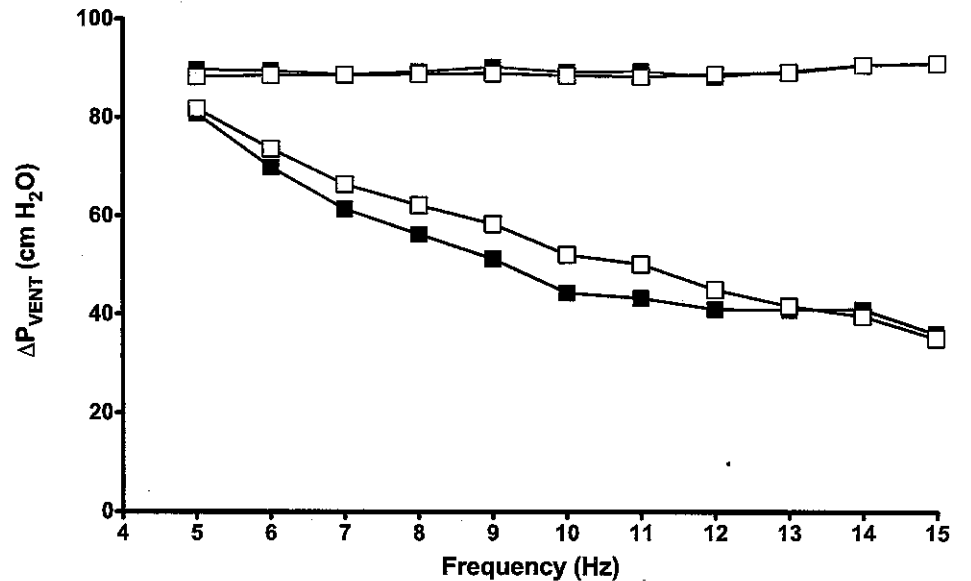
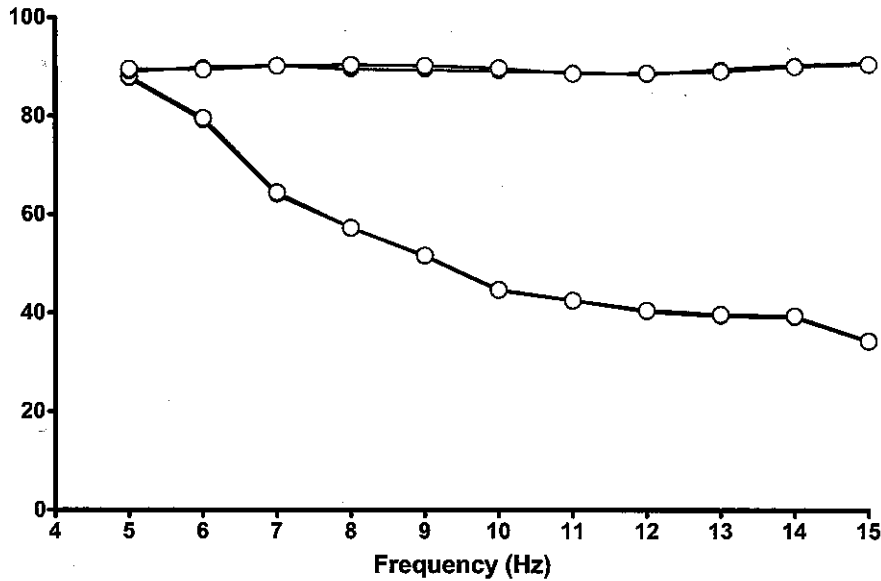
OSM Figure 1. Relationship between frequency and ΔP_{VENT} for the SM3100 (red) and the VN500 (blue) for ETT sizes 2.5mm (circles; **Panels A and C**) and 3.5mm (squares; **Panels B and D**) at a test lung C_{RS} of 1.0 mL/cm H₂O (open circles and squares) and C_{RS} 2.0 mL/cm H₂O (filled circles and squares). **Panels A and B** shows data using an I:E ratio 1:2 and **Panels C and D** I:E ratio 1:1.

OSM Figure 2. Relationship between frequency and V_{THF} for the SM3100 (red) and the VN500 (blue), both at I:E ratio 1:2, for ETT sizes 2.5mm (circles; **Panel A**) and 3.5mm (squares; **Panel B**). Test lung C_{RS} set at 1.0 mL/cm H₂O (open circles and squares) and 2.0 mL/cm H₂O (filled circles and squares).

OSM Figure 3. Percentage difference in V_{THF} generated by the SM3100 and VN500 at different frequencies in a test lung with C_{RS} 1.0 mL/cm H₂O for a 2.5 mm ETT. Closed triangles represent data for I:E ratio of 1:2 and open triangles 1:1.

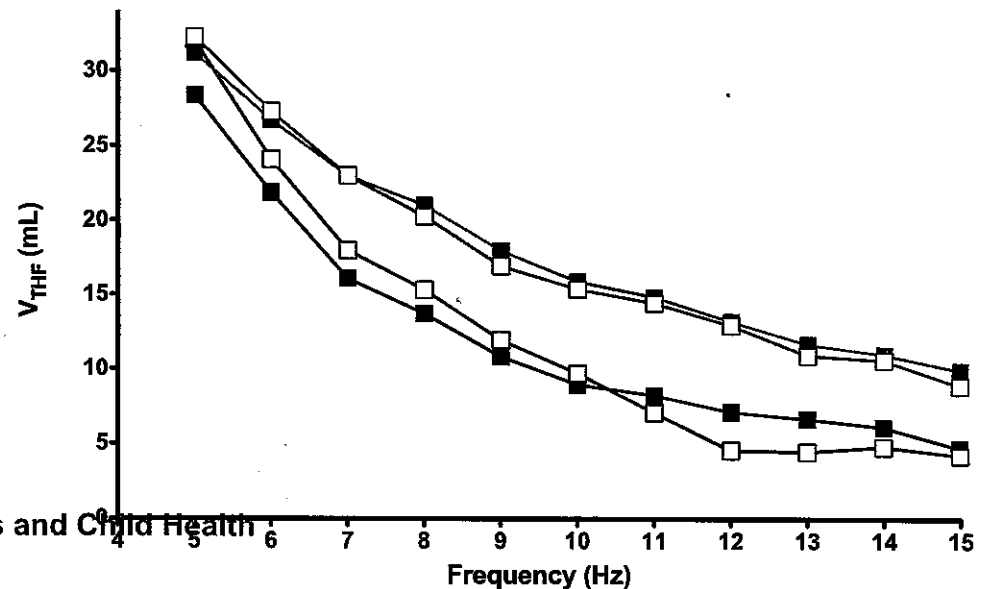
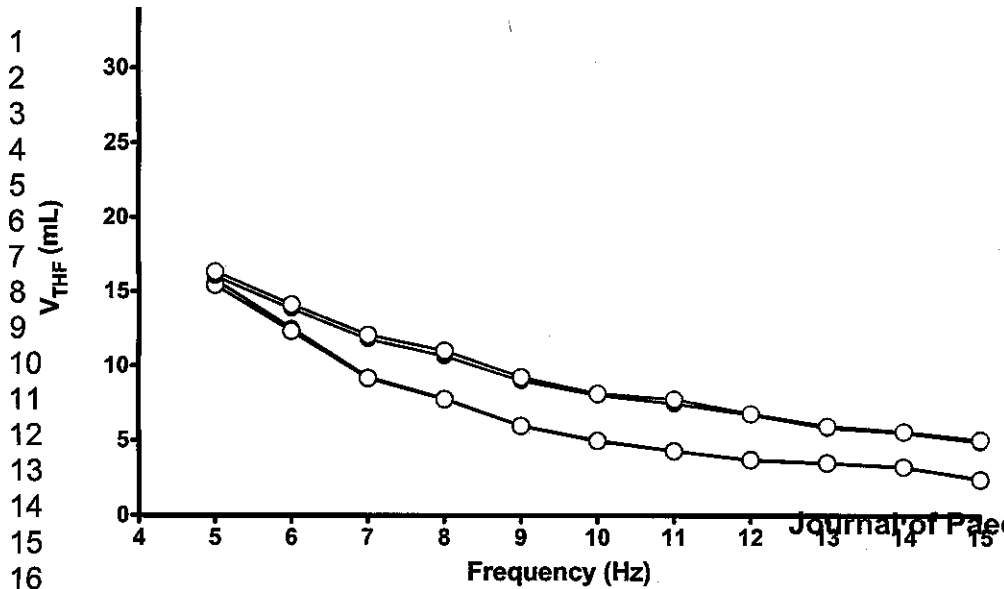
OSM Figure 4. Relationship between frequency and ΔP_{TRACH} for the SM3100 (red) and the VN500 (blue) at a test lung C_{RS} of 1.0 mL/cm H₂O (open circles) and C_{RS} 2.0 mL/cm H₂O (filled circles) with a 2.5 mm ETT. Data from Figure 3 represents the differences in ΔP_{TRACH} at each frequency between SM3100 and VN500.

1
2
3
4
5
6
7
8
9
10
11
12
13
14
15
16
17
18
19
20
21
22
23
24
25



OSM Figure 2A

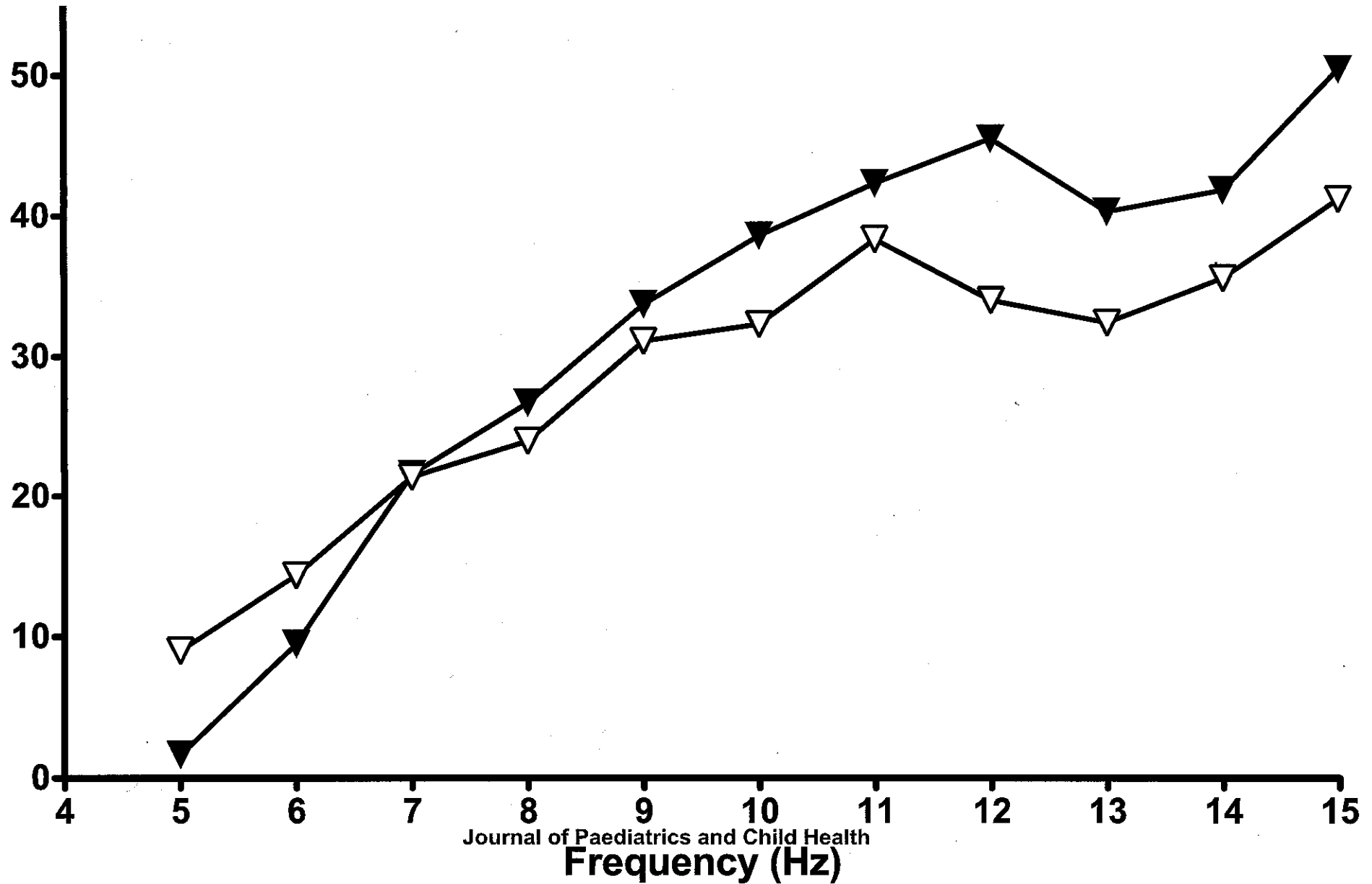
OSM Figure 2B



1
2
3
4
5
6
7
8
9
10
11
12
13
14
15
16
17

OSM Figure 3

1
2
3
4
5
6
7
8
9
10
11
12
13
14
15
16
17
18
19
20
21
22
23
24
25
26
27
28
29
30
31
32
33
34
35
36
37
38

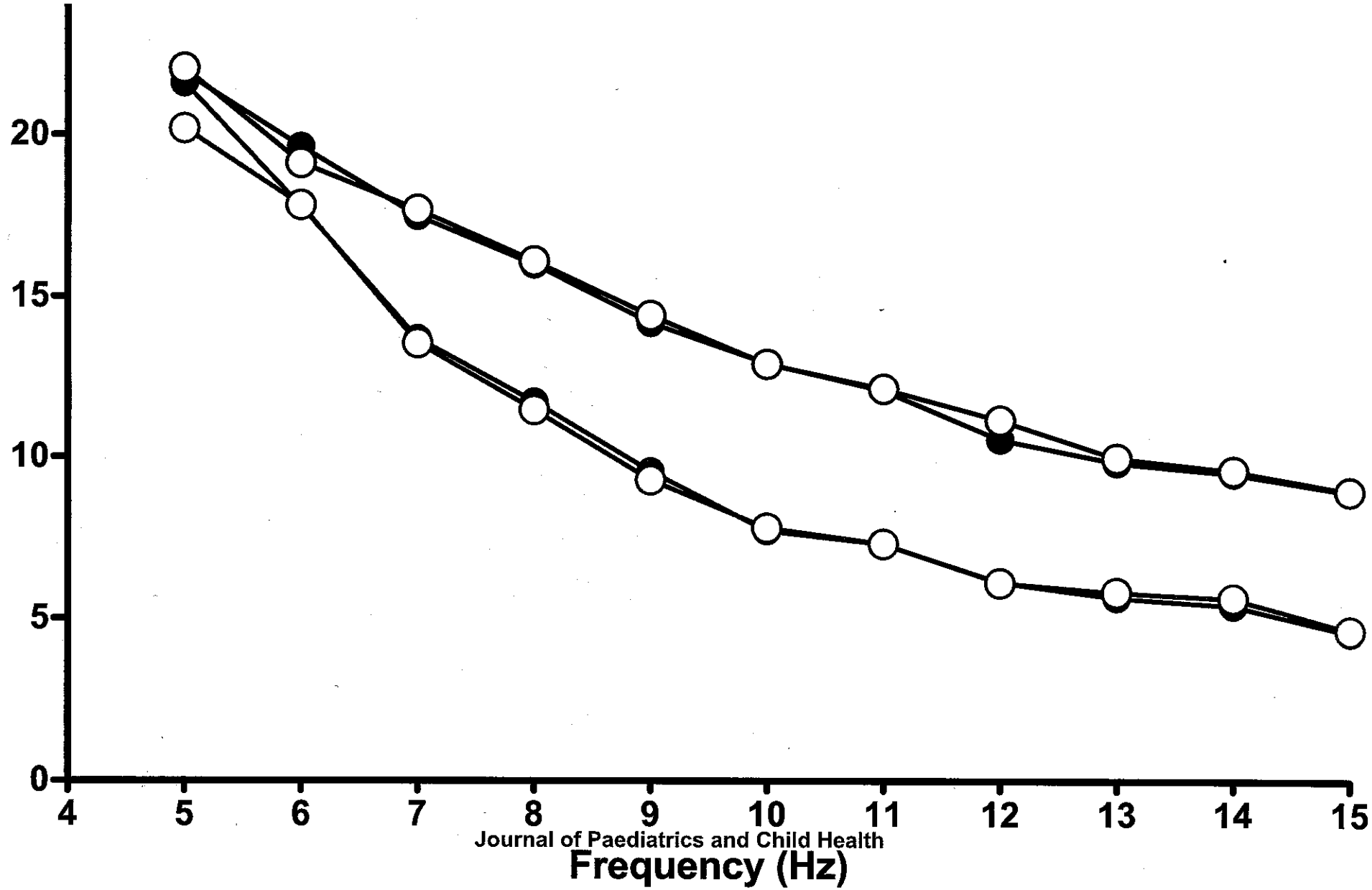


Frequency (Hz)

OSM Figure 4



1
2
3
4
5
6
7
8
9
10
11
12
13
14
15
16
17
18
19
20
21
22
23
24
25
26
27
28
29
30
31
32
33
34
35
36
37
38



Frequency (Hz)